Paper-Based Microfluidics

International Edition: DOI: 10.1002/anie.201411508
German Edition: DOI: 10.1002/ange.201411508

Paper-Based Inkjet-Printed Microfluidic Analytical Devices

*Kentaro Yamada, Terence G. Henares, Koji Suzuki, and Daniel Citterio**

Keywords:
analytical methods · bioassay · inkjet printing · microporous materials · sensors

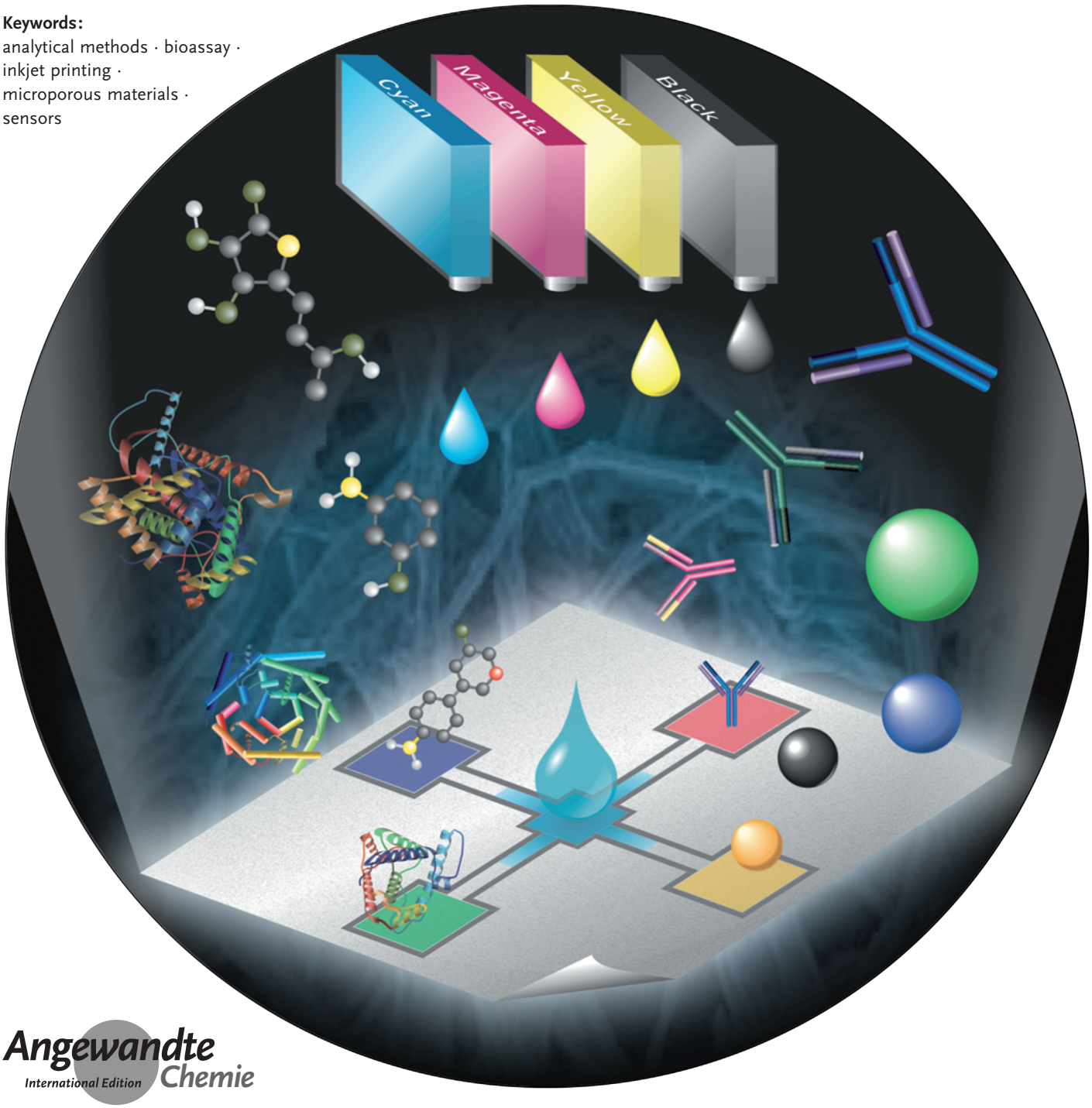

Rapid, precise, and reproducible deposition of a broad variety of functional materials, including analytical assay reagents and biomolecules, has made inkjet printing an effective tool for the fabrication of microanalytical devices. A ubiquitous office device as simple as a standard desktop printer with its multiple ink cartridges can be used for this purpose. This Review discusses the combination of inkjet printing technology with paper as a printing substrate for the fabrication of microfluidic paper-based analytical devices (μPADs), which have developed into a fast-growing new field in analytical chemistry. After introducing the fundamentals of μPADs and inkjet printing, it touches on topics such as the microfluidic patterning of paper, tailored arrangement of materials, and functionalities achievable exclusively by the inkjet deposition of analytical assay components, before concluding with an outlook on future perspectives.

From the Contents

1. Introduction

Microfluidic paper-based analytical devices, or in short μPADs, first described by Whitesides and co-workers in 2007, are analytical devices with microfluidically patterned paper as their main component.[1] Very simplified, they can be regarded as either a paper variant of conventional microfluidics or an advanced version of classical dipstick tests. The philosophy behind μPADs is to provide extremely low-cost, disposable, simple to use, analytical devices applicable in low-resource settings, such as those encountered in developing countries, in field analysis, or in private homes, where technical infrastructure is limited and trained experts are absent. In their ideal form, μPADs are self-standing analytical systems with all the components necessary to perform an analytical assay (e.g. sample transport, sample pretreatment, assay reagents, signaling system) integrated into the device (Figure 1). Although the majority of research activities into μPADs are targeting healthcare-related diagnostics, where the impact of cost reduction and simplicity is deemed to be highest, other fields of applications, such as environmental monitoring, explosives detection, or screening for food and beverage contamination are continuously joining the list.[2]

The primary motivation for replacing glass or polymer substrates of conventional microfluidics with paper is the requirement for a low-cost, abundantly available, and disposable material.[3] In addition, the physical-chemical properties of cellulosic paper make it an extremely versatile material that is ideally suited for application to microfluidics. Liquid transport in μPADs entirely relies on capillary flow, thus making external pumping unnecessary. Additionally, the chemical composition of paper and its high surface to volume ratio allows for the simple physical immobilization of reagents required in an analytical assay. These functions can not be achieved so straightforwardly and simply with more "high-tech" materials. On the other hand, the motivation for adding microfluidic features to classical paper dipstick tests is to increase their functionality and performance. Spatial separation of sample introduction and signal detection allows for splitting the sample into different assays,

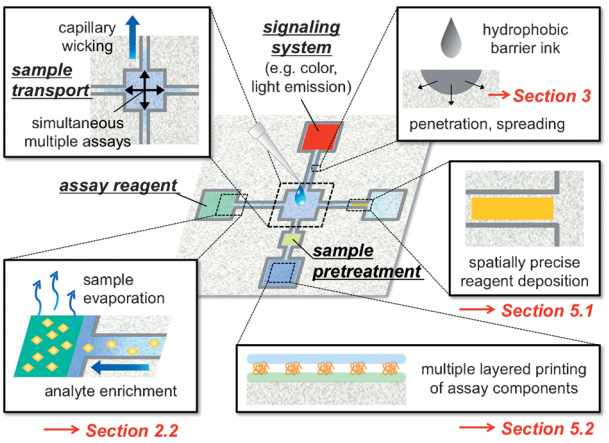

Figure 1. Schematic representation of a microfluidic paper-based analytical device (μPAD) illustrating its multifunctional character.

on-device sample pretreatment, and time delays for incubation, to mention a few options not available with dipstick assays.

In its very basic principle, an inkjet printer performs the contactless dispensing of picoliter-sized droplets of liquids (inks) onto a user-defined position of a substrate. Inks can incorporate a variety of materials going beyond classical dyes and pigments, and so inkjet printing has become an essential tool in industrial mass production[4] and for printed electronics.[5] In chemistry, biology, and life sciences, inkjet printing first became routinely used for the deposition of nucleic acids in the fabrication of DNA chips.[6]

Knowing about the printability of biomolecules and working with paper substrates should have made it downright

[*] M. Eng. K. Yamada, Prof. Dr. T. G. Henares, Prof. Dr. K. Suzuki, Prof. Dr. D. Citterio
Department of Applied Chemistry, Keio University
3-14-1 Hiyoshi, Kohoku-ku, Yokohama 223-8522 (Japan)
E-mail: citterio@applc.keio.ac.jp

"obvious" to refer to inkjet printing for the development of μPADs. Nevertheless, the first μPADs were obtained by photolithographic patterning of filter paper, followed by manual deposition of assay reagents.[1] In 2008, our research group demonstrated for the first time that inkjet printing technology is a viable approach for both the microfluidic patterning of paper substrates and the deposition of assay reagents.[7]

Although still relatively young, the topic of microfluidic paper-based analytical devices has been reviewed multiple times and the list of references given here is probably not complete.[2,3,8–23] Similarly, there are several reviews on the application of inkjet printing for material deposition.[5,24–30]

Whereas previous reviews mostly focused on the analytical applications of μPADs, the purpose of the present Review is to discuss the basics, strengths, and weaknesses related to the application of inkjet printing technology for the fabrication of μPADs. Since research on inkjet-printed μPADs is a very multifaceted field, the literature references included here are related to areas such as analytical chemistry, inkjet printing technology, physical chemistry, paper chemistry, material chemistry, and polymer chemistry.

2. Fundamentals

2.1. From Microfluidic Analytical Devices to μPADs

In the 1980s, the trend to miniaturization, promoted by technological advances in microscale processing, gave birth to microfluidic analytical devices, referred to as "μTAS" (miniaturized/micro total analysis systems)[31–33] or "lab-on-chip" (LOC) devices. The integration of process steps reaching from sample transport, sample pretreatment, separation, and analyte detection on a single platform is in line with the demand for more simple and precise analytical assays. As a positive "side effect", miniaturization of analytical systems brought along the advantage of dramatically reduced sample volumes and lower consumption of reagents.

As a consequence of their efficiency, speed, and operational simplicity, microfluidic analytical devices have been suggested as ideal tools for clinical diagnostics outside of hospital laboratories.[34] However, despite this perspective, we are still far from the situation that every person monitors their health conditions at home using an LOC device.[35] The reason is that the advantageous features outlined above are for many microfluidic analytical devices only partially reduced to practice. The step away from the lab bench often remains a challenge.[36] One significant hurdle with LOC devices is the size, complexity, and costs of fluid handling.[37] A second one is the requirement for the user to introduce a number of reagents needed for the assay.[38]

A well-known analytical technology that has solved the problem of liquid transport in a very simple way is paper chromatography.[39] Paper, as a microporous hydrophilic material, is able to wick aqueous liquids. The first time that this property was used to control the flow of liquid was in a piece of filter paper patterned with a fluidic channel defined by a barrier of solid wax to simplify paper chromatography (Figure 2).[40] Although with that report in 1949 Müller and Clegg laid the foundation for the realization of fluidic devices made from paper, it was only six decades later that the concept of microfluidic paper-based analytical devices was introduced[1] and coined as "μPADs",[41] which has in the meantime grown into a thriving research area of analytical chemistry (Figure 3).

Kentaro Yamada received his B. Eng. and M. Eng. from Keio University in 2013 and 2014, respectively. He is now carrying out PhD research, focusing on the development of inkjet-printed microfluidic paper-based analytical devices.

Terence G. Henares received his PhD from the University of Hyogo in 2008. After postdoctoral studies at the Population Council Center for Biomedical Research in New York, and at Osaka Prefectural University, he became a Project Associate Professor at Keio University. His research interests are in the development of microfluidic analytical devices.

Koji Suzuki received his PhD in 1982 from Keio University. He became a faculty member there as a Research Associate in 1982, Assistant Professor in 1988, Associate Professor in 1993, and full Professor in 1998. From 1990 to 1992, he was a Guest Professor at the Swiss Federal Institute of Technology (ETH), Zurich. Since 2015, he serves as the President of the JSAC. His research focuses on chemical and biochemical sensors based on functional molecule creation.

Daniel Citterio received his PhD in Chemistry in 1998 from the Swiss Federal Institute of Technology (ETH) in Zurich. After postdoctoral research at Keio University, he became a Research Associate at ETH in 2002. Following post-graduate studies and work at Ciba Specialty Chemicals, he returned to Keio University in 2006. In 2009 he became a tenured Associate Professor and in 2014 Professor in Analytical Chemistry. His research interests are the development of low-cost analytical devices and the development of functional molecules for chemical sensing.

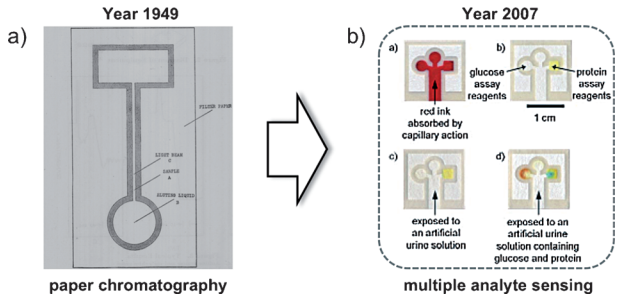

Figure 2. Pioneering studies on microfluidic paper-based analytical devices: a) first microfluidically patterned filter paper for paper chromatography (adapted from Ref. [40] with permission. Copyright 1949 American Chemical Society) and b) first μPAD for simultaneous multiple analyte assay (adapted from Ref. [1] with permission. Copyright 2007 Wiley-VCH Verlag GmbH & Co. KGaA, Weinheim).

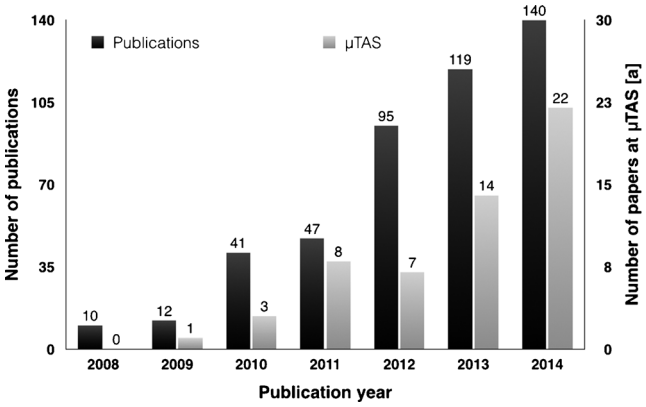

Figure 3. Number of publications/conference papers related to μPADs. [a] Yearly international conference on miniaturized systems for chemistry and life sciences.

2.2. Conventional Microfluidics and μPADs: Similarities and Differences

The most important common feature of both conventional polymer/glass- and paper-based microfluidic devices is the minimal consumption of reagents and samples and the ability for multiplexed analysis. The differences between the two systems arise from the type of microfluidic channels. Whereas conventional microfluidics have hollow closed channels, their paper counterparts rely on porous open channels. Apparently, the fluid flow for both devices is laminar.[2] For simplicity, a conventional microfluidic device can be treated as a "single capillary" system, where the amount of sample is defined by the channel dimension, which is on the order of sub-microliter. The analysis of such miniscule volumes requires sophisticated detectors, such as for example a fluorescence microscope. Furthermore, if a sub-milliliter sample is analyzed in a continuous flow, a pump system is needed. This requires in most cases bulky instrumentation and a trained expert for operation. In contrast, the porous nature and open channels of a μPAD can be simply considered as a device possessing many different capillaries with different radii. As a consequence, continuous flow of fluid occurs because of the wicking property of paper, and the constant fluid evaporation acts as a negative pressure pump. Thus, simple fluid handling in a pump-free fashion is anticipated. This kind of dynamic fluid flow can be used for analyte enrichment and signal amplification.[42] A drawback of using paper as a substrate is the nonspecific adsorption of molecules onto cellulose, which diminishes the amount of analyte reaching the assay area and has to be compensated by calibration. Finally, most μPADs require only simple modes of detection (e.g. colorimetry) that are achievable with daily use devices such as a camera (e.g. mobile phone, smartphone) or a scanner.

2.3. Paper Substrates

Filter paper and chromatography paper are the most widely used substrates for μPADs. They are composed of pure cellulose, while many other papers contain structure-reinforcing additives[23] that are potentially detrimental in analytical assays. For example, surface coatings can prevent deposited components from diffusing into the paper matrix. Brighteners used to improve the whiteness cause a high background emission in fluorescence-based detection.[43]

On the other hand, filter paper and chromatography paper do not undergo treatment with such additives, and almost all impurities from the raw material (lignin, etc.) are removed after full bleaching. Cellulose is the primary component, with abundant hydroxy groups (-OH) and a few carboxylic acid groups (-COOH) present on the fiber surface.[44] They can serve as scaffolds for the immobilization of substances required in a μPAD. It has been reported that positively charged compounds are electrostatically adsorbed onto the slightly anionic surface of cellulose, while non-ionic or anionic ones are not.[45] In addition, proteins also show slight electrostatic interaction with cellulose through their cationic regions. Covalent bonding is often exploited for the more robust attachment of biomolecules. Since the hydroxy groups of cellulose are not sufficiently reactive under mild conditions, activation by derivatization to aldehyde[46] or epoxy groups,[47] introduction of poly(carboxybetain) followed by EDC/NHS chemistry,[48] and modification by divinyl sulfone[49] have been demonstrated to covalently immobilize various biomolecules onto paper (Figure 4). In some cases, the "scaffolds" not only bridge the paper substrate and reagents to be immobilized, but also reduce the nonspecific adsorption of biomolecules onto paper.

2.4. Basic Concept and Methods of Inkjet Printing

The historical background of inkjet printing has been chronicled by Le in terms of technological advancements.[50] The following section focuses on the fundamentals of inkjet printing, such as types of printers and ink printability.

In terms of application, inkjet technology is divided into two major categories: drop-on-demand (DOD) and continuous inkjet (CIJ). All of the common desktop printers and all laboratory-relevant inkjet printing systems rely on DOD technology. In contrast to the CIJ mechanism with a contin-

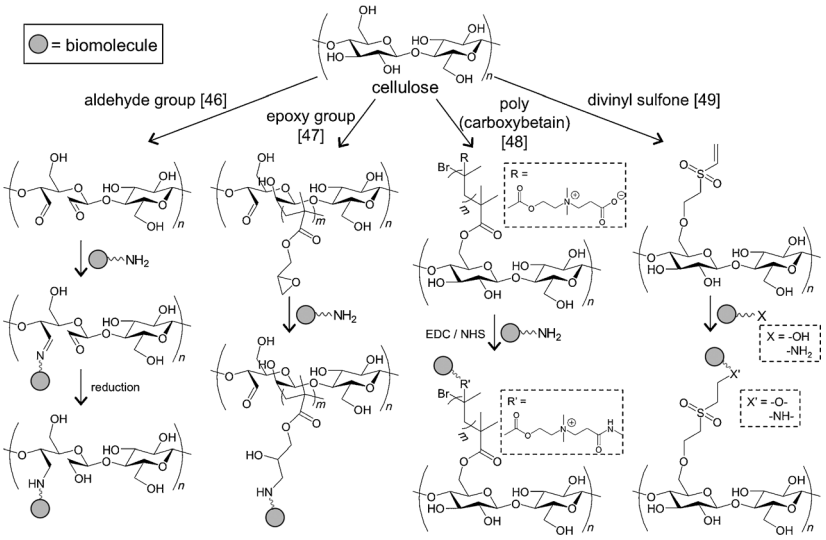

Figure 4. Strategies applied for the activation of cellulosic hydroxy groups and the covalent attachment of biomolecules.

uous ejection of fluid, the jetting of ink onto the substrate only occurs when it is needed, as implied by the term "drop-on-demand". DOD inkjet printing is divided into four modes of actuation: piezoelectric, thermal, electrostatic, and acoustic. At present, only the piezoelectric and thermal methods are routinely utilized. Figure 5 demonstrates the process of fluid

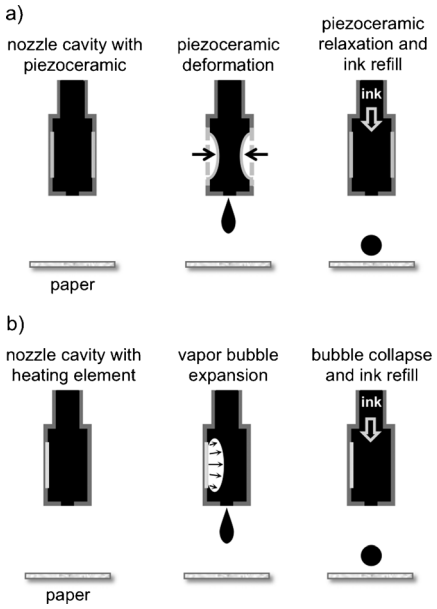

Figure 5. Basic working principle of drop-on-demand (DOD) inkjet printing: a) piezoelectric inkjet and b) thermal inkjet.

jetting for these two DOD printers. Initially, the ink inside the cavity experiences an increase in pressure arising from a piezoceramic deformation (piezoelectric; Figure 5a) or a vapor bubble expansion (thermal; Figure 5b). Rapid expansion of a vapor bubble is achieved by superheating the ink by a heat pulse applied for about 2 μs.[51] For water-based inks, heating is around 200–300 °C.[50] Once the ink is ejected, the bubble rapidly collapses, which creates a vacuum that allows the automatic refilling of ink in the cavity from the reservoir (ca. 80–300 μs filling time depending on the print head's channel design and ink properties). The jetting time is estimated to be about 10 μs, which involves expansion and collapse of the vapor bubble.[50]

The ink is an essential component in the overall inkjet printing process, thus making its properties decisive for success or failure. Its physico-chemical properties dictate the resolution, drop velocity, and reliability of printing. Various mathematical expressions such as the Reynolds (Re), Weber (We), and Ohnesorge (Oh) numbers [Eq. (1)] have been utilized to evaluate the practical printability of fluids under DOD conditions.[52–54]

$$Z = Oh^{-1} = Re/We^{1/2} = (\gamma \rho a)^{1/2}/\eta \quad (1)$$

Here, $Re = v\rho a/\eta$ and $We = v^2\rho a/\gamma$, where ρ, γ, and η are the density, surface tension, and viscosity of the fluid, respectively, while v is the drop ejection velocity and a the nozzle radius. It has been reported that to generate a stable droplet, the Z value should be $0.67 < Z < 50$.[54] A Z value higher than 50 could result in the formation of satellite droplets trailing the primary droplet, which has a negative impact on print resolution. Z values lower than 0.67 could lead to a strong contribution of viscous dissipation, finally preventing droplet ejection.[55] This approximation has been modified and could be further modified to suit the printability of inks with more challenging rheological properties.[53,54,56] All of these numerical and experimental investigations are geared towards attaining stable, satellite-free printable inks that form well-defined patterns without clogging the nozzle. To achieve the required ink properties, it is often necessary to adjust the viscosity and surface tension by modifiers. Typically, the range of surface tension for both thermal and piezoelectric inkjet printing inks is 28–40 $mN\,m^{-1}$.[57] Thermal inkjet enables printing with lower ink viscosity (minimal 1–1.5 cP, typically < 3 cP), which often allows working with simple aqueous solutions without modifiers. However, the piezoelectric method (minimal 5–10 cP, typically < 20 cP) generally requires the addition of viscosity modifiers when using water-based inks.[27,58,59] These ranges should serve as guides, rather than requirements, and ink adjustments are always recommended.

3. Microfluidic Patterning of Paper Substrates

In this section, major methods for patterning channels in μPADs are briefly discussed, with the exception of inkjet printing, to which the following Section 4 is devoted. Figure 6 gives an overview of various channel fabrication principles. In the simplest case, patterning can be achieved by cutting the

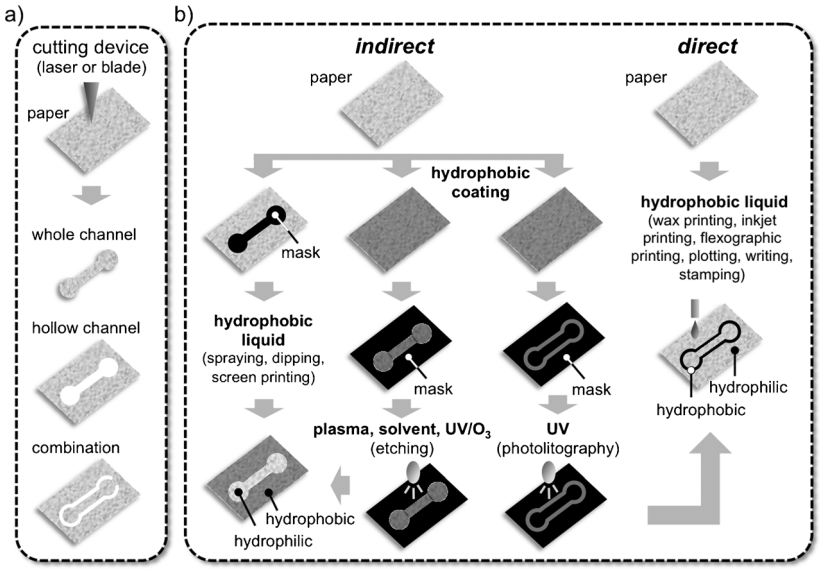

Figure 6. Methods to create microfluidic channels on paper substrates: a) mechanical cutting of paper and b) treatment with hydrophobic materials.

paper[60–62] (Figure 6a), which is not further discussed here. A more widely used approach is treatment with a hydrophobic material (Figure 6b). The hydrophobic modification approaches can be subdivided into indirect and direct patterning methods. Indirect patterning methods rely on the use of a mask to project the shape of the microfluidic channel structure on the paper. On the other hand, direct methods involve the deposition of hydrophobic compounds onto selected positions of the paper substrate in such a way as to define the structure of the flow channel.

The main objective in the fabrication of microfluidic channels on paper substrates by hydrophobic treatment is to obtain a contrast between the hydrophobic barrier and the hydrophilic flow channel. The hydrophobically impregnated areas define the dimensions of the channel (Figure 6b). The porosity and surface composition of cellulose fibers are two important characteristics for the covalent or noncovalent hydrophobic treatment of the substrate. Porosity allows the penetration and filling with liquid through the void spaces. There are three types of pores found in cellulose networks: the voids between fibers, the retained lumen, and the inherent pores of the fiber walls.[23]

One strategy to fabricate a hydrophilic microstructure on paper is to fill the void spaces with a hydrophobic material, thereby creating a barrier to aqueous liquids. Hydrophobic materials applied for this purpose can, for example, be a solid that melts at a specified temperature or a solution of a hydrophobic polymer in an organic solvent. In their liquid state, both materials are able to penetrate into the porous network, and a hydrophobic barrier is obtained once the material solidifies at room temperature or its solvent evaporates. This approach is a noncovalent treatment of the cellulose.

Another possible way to define a hydrophilic channel on a paper substrate is to covalently modify the cellulose fibers. The presence of hydroxy (-OH) or carboxylic acid (-COOH) groups renders them suitable for chemical modification,[63] a feature that is regularly made use of in paper manufacturing. A class of compounds often applied are the so-called "sizing" agents such as alkyl ketene dimer (AKD), alkenylsuccinic anhydride (ASA), or rosin.[23] They are hydrophobic reagents that lower the surface energy of the cellulosic material, thereby improving the resistance to water as a result of an increase in surface hydrophobicity.[64] AKD has been utilized in particular for the microfluidic patterning of paper by inkjet printing and will be discussed in Section 4.

In practice, the microfluidic patterning of μPADs can be achieved by using various techniques such as photolithography,[1,41,65–68] etching,[7,67,69,70] writing,[71–74] dipping,[75] printing,[7,70,72,74,76–85] stamping,[86,87] and spraying,[88] with each approach using its corresponding hydrophobic reagent to create the hydrophobic barriers (Table 1).

One disadvantage of photolithography is the exposure of the entire paper substrate (including those areas to be converted into hydrophilic channels) to solvents and hydro-

Table 1: Hydrophobic materials used for the microfluidic patterning of paper substrates.

Technology	Hydrophobic material
Indirect patterning	
photolithography	SU-8 photoresist,[1,41,65,66] octadecyl-trichlorosilane,[67] acryloxy-terminated/acrylate-based polymer blend[68]
etching	polystyrene,[7] octadecyltrichlorosilane,[67] alkyl ketene dimer,[69] hydrophobic sol-gel[70]
spraying	acrylic lacquer[88]
screen printing	polystyrene,[76] wax[85]
dipping	wax[75]
Direct patterning	
wax printing	wax[74,77,81]
plotting	poly(dimethylsiloxane)[82]
flexography	polystyrene,[79] poly(dimethylsiloxane)[83]
writing	crayon,[71,74] water-based marker,[72] permanent marker[73]
stamping	paraffin,[86] wax[87]
inkjet printing	polystyrene,[7] hydrophobic sol-gel,[70] silicone,[78] alkyl ketene dimer,[80] polyacrylate[84]

phobic reagents, and the relatively large consumption of hydrophobic reagents required to treat the whole paper substrate. It was, therefore, a practical consequence to search for maskless direct patterning strategies, where a small amount of hydrophobic material is specifically deposited solely to confine the hydrophilic channel structure, while keeping the rest of the paper unadulterated.

One of the most commonly used techniques to achieve minimal consumption of hydrophobic material is to utilize printing. In terms of μPAD fabrication, there are numerous reasons that make printing an appealing solution: 1) adaptable for mass production, 2) cost-effective, 3) reproducible, and 4) simple. Recently, several printing techniques have been adapted for this purpose, such as screen printing,[76,85] flexographic printing,[79,83] and digital printing.[7,70,72,74,77,78,80,81,84] Digital printing enjoys great popularity and wide use, since it can directly relay image information from a computer onto the print substrate, without the costly and time-consuming conversion of electronic data into printing plates, masks, or screens. Image transfer from the printer onto the surface of the paper substrate is achieved by digitally controlled direct deposition of ink. Of the digital printing techniques, wax and inkjet printing are the preferred methods to pattern paper, because of their ease of use and their commercial ubiquity. Various research groups have demonstrated the use of wax printed on filter paper for the creation of two- (2D) and three-dimensional (3D) microfluidic structures, including hemi- and fully enclosed channels.[74,77,81] A wax printer transfers molten wax onto the paper substrate, where it immediately solidifies upon contact. Apparently, this prevents penetration of the hydrophobic wax into the cellulose network. However, by application of heat (> 120 °C) to the printed paper substrate in an oven or on a hotplate, the deposited wax is re-liquefied and wicks into the void spaces of the cellulose network, finally forming a solid wax barrier at room temperature.

Characterized by its simplicity and speed, wax printing is an excellent technique to obtain the hydrophobic barriers required to define a microfluidic structure on paper substrates. However, the fabrication of a μPAD is not completed by the creation of microfluidic patterns. To obtain a fully operational analytical device, the presence of further functional materials that enable analytical operations such as sample pretreatment, separation, analyte signaling, and other functions is required. Therefore, the use of a single printing technology that allows to deposit both the materials used to define hydrophilic channels and the materials to perform analytical assays is a significant advantage towards the efficient fabrication of complete μPADs.

4. Paper Patterning by Inkjet Printing

4.1. Inkjet Etching

Our research group demonstrated the first use of sequential inkjet printing for both the patterning of microfluidic channels and the deposition of assay reagents in the fabrication of a paper-based analytical device (Figure 7) for simultaneous measurements of multiple analytes.[7] The workhorse of this μPAD patterning technique is based on "inkjet etching", a concept that was first demonstrated for the etching of holes and trenches in polymer films.[89,90] Inkjet etching applied to a filter paper substrate relies on the dissolution of solid polymeric material upon local exposure to the jetted solvent ink, thus allowing the reappearance of the originally hydrophilic cellulose network (Figure 7a). In this approach, the paper substrate is first converted into an entirely hydrophobic material by soaking it into a polystyrene solution (1.0 wt% in toluene) and drying it at room temperature for 2 h. The hydrophobic paper is then exposed to the inkjet printing of picoliter volumes of toluene, thereby leading to a channel width of about 550 μm (Figure 7b). It was observed that 10 printing cycles registered an excellent patterning reproducibility in terms of control of the size of the patterned structure and homogeneity of channel wetting. Although the inkjet-etching patterned μPADs allowed the successful simultaneous analysis of protein, glucose, and pH (Figure 7c),[7] and in later work has been applied to an immunoassay (both examples are discussed in more detail in Section 5),[91] the toluene used as the ink was considered a disadvantage to the user and environment, because of its classification as a flammable and volatile organic compound (VOC). Therefore, the focus was shifted to a more environmentally friendly approach to inkjet-based μPAD fabrication. First, attempts were made to replace toluene with a "greener" solvent such as limonene (component of degreasers and certain cosmetics), but the microfluidic channels formed were not well defined. With its significantly lower vapor pressure compared to toluene, the ink-jetted limonene remained in contact with the polystyrene for too long a period of time, thereby resulting in an uncontrolled and extended etching of the hydrophobic polymer. Furthermore, both toluene and limonene required a customized printer for jetting, since their high dissolving power is detrimental to the plastic components used in desktop inkjet printers. In addition, the inkjet etching

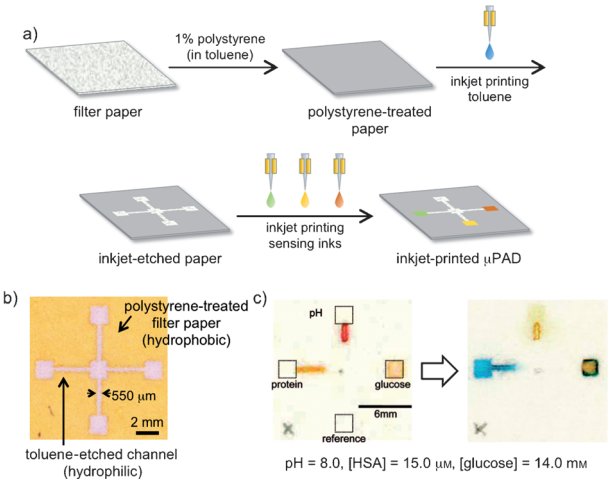

Figure 7. Channel patterning by inkjet etching: a) fabrication principle, b) photograph of a patterned channel on filter paper, and c) colorimetric response after sample application (adapted from Ref. [7] with permission. Copyright 2008 American Chemical Society).

approach suffers from the same drawback as the previously discussed photolithography and other mask-based patterning techniques, since it requires a relatively large amount of hydrophobic material to initially hydrophobize the paper substrate in its entirety. Finally, similar to photolithography, all areas of the paper substrate, including the final hydrophilic microfluidic structures, get exposed to solvents and other chemicals at some point of the patterning process, with potentially unknown effects on the analytical assays to be performed on the devices.

4.2. Direct Inkjet Printing of Hydrophobic Barriers

To overcome these shortcomings, a UV-curable ink for channel patterning by a desktop inkjet printer was developed (Figure 8).[84] In this case, the ink is a pre-polymer solution composed of octadecyl acrylate (monomer), 1,10-decanediol

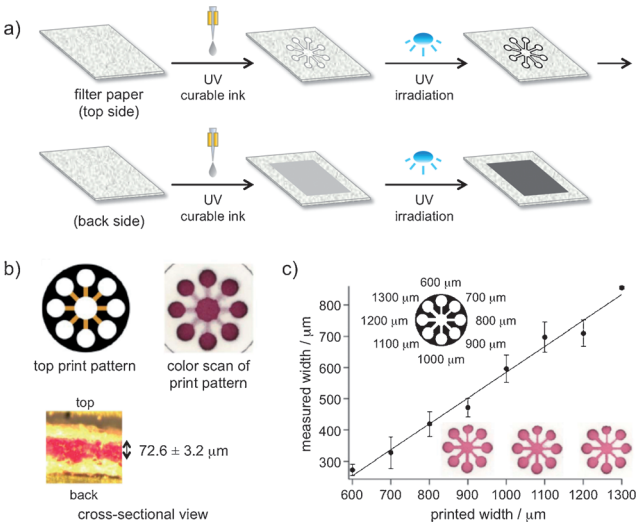

Figure 8. Microfluidic channel patterning by UV-curable inkjet ink: a) fabrication principle, b) 3D-printed fully enclosed channel in a single sheet of filter paper, and c) relationship between printer set and actual channel width. Adapted from Ref. [84] with permission from The Royal Society of Chemistry.

diacrylate (cross-linker and solvent), and 2,2-dimethoxy-2-phenylacetophenone (photoinitiator). Besides their highly hydrophobic character, long alkyl chain acrylates have very low volatility. This prevents rapid evaporation, which is essential for allowing sufficient time for penetration into the paper substrate and for polymerization without loss of the UV-curable ink. Polymerization is initiated by exposure to UV light (60 s), which leads to the formation of a hydrophobic interpenetrating polymer within the cellulose network. Similar to the previously discussed wax printing approach, ink deposition requires a single printing cycle while regulating the amount of ink by changing the transparency settings of the graphical elements defining the borders of the microfluidic channel in the computer software.

The fabrication method is shown in Figure 8a. Both sides of the paper were printed with UV-curable ink, which allows the formation of different channel structures such as hemi-channels or 3D channels on a single piece of paper (Figure 8b). Hydrophilic channels as narrow as 272 μm have been achieved with this patterning method (Figure 8c). The microfluidic structures maintained their wicking properties for at least 6 months when stored at room temperature, and for a minimum of 72 h at 50 °C. This patterning strategy has been successfully applied for an enzyme assay (H_2O_2) and an antibody-free bioassay of tear fluid (lactoferrin).[84,92]

Aside from UV-curable inks, other inks that have been used for direct inkjet-based channel patterning of μPADs are the paper-sizing agent alkyl ketene dimer (AKD),[80,93,94] silicone,[78] hydrophobic sol-gel,[70] and aqueous fluoroacrylic copolymer dispersion.[95] Among these inks, AKD is the most facile to use, since, as already discussed in Section 3, it has a long history as a paper-sizing agent and is, therefore, commercially available. As shown in Figure 9a, the lactone

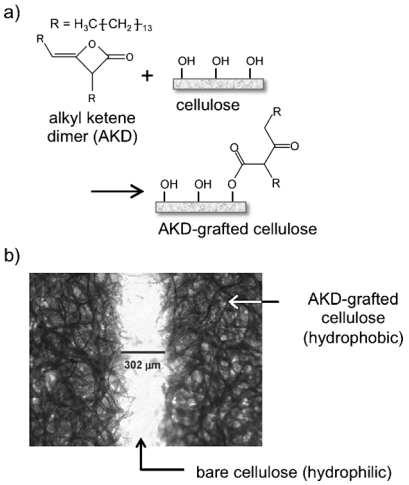

Figure 9. Inkjet-printed alkyl ketene dimer (AKD) for channel patterning: a) grafting of cellulose by AKD and b) micrograph of a printed channel (adapted from Ref. [80] with permission. Copyright 2010 Elsevier B.V.).

group of AKD reacts with cellulosic hydroxy residues through an esterification reaction, thereby creating a demarcation between the hydrophobic (AKD printed) and hydrophilic (native filter paper) region of the μPAD. For inkjet printing applications, AKD is dissolved in heptane, which has a high vapor pressure, thus, easily evaporates upon printing. The final step of the patterning process is a curing step at 100 °C for 8 min. Microfluidic channels of about 300 μm width have been patterned with this technique (Figure 9b).

All of the inkjet-based patterning approaches discussed lead to hydrophobic barriers that are fully compatible with aqueous sample liquids. However, some real samples may contain reagents that could compromise the integrity of a barrier. For example, when analyzing cell lysates containing a relatively high concentration of surfactants, it has been reported that AKD-printed barriers are breached.[70,78] Leaking also occurs with wax-printed structures.[96] With inkjet-printed barriers based on UV-ink, leaking has been observed with solutions that have a surface tension lower than

30 mN m^{-1}.[84] However, hydrophobic barriers with inkjet-printed silicone and hydrophobic sol-gel methylsilsesquioxane (MSQ) maintained their integrity in the presence of surfactants and several organic solvents.[70,78]

This section has shown that inkjet printing has become established as a method to create microfluidic structures in μPADs. All of the introduced approaches have their strengths and weaknesses in terms of speed, simplicity, achieved resolution, availability of reagents, applicable printing equipment, and chemical resistance of barriers. The choice available should be regarded as an opportunity to select the method that is most suitable for a specific application and available printing equipment. It also has to be stated that, at present, none of the inkjet-based approaches is probably able to compete with wax printing as far as speed on a laboratory prototypical scale is concerned. However, the possibility to inkjet-print additional unit operation(s) on the same μPAD is a very strong argument in favor of this printing technique. This is particularly true considering the fact that the inkjet printing of various functional materials was already established way before the development of modern μPADs.[28] Thus, it is only natural to unify the creation of paper-fluidic structures with the deposition of other functional materials by using a single printing technique.

5. Assay Reagent Deposition by Inkjet Printing

In this section, the use of inkjet printing is discussed in terms of the deposition of assay reagents. An overview of general assay types, printed functional materials, and general ink composition is summarized in Table 2. The three principal assay methods listed represent almost all the chemical or biochemical assays currently reported for inkjet-printed μPADs, which means that the majority of μPADs are based on known and established assay principles.

Table 3 provides a more-detailed overview of paper-based analytical devices where inkjet printing is involved in at least one fabrication step: in microfluidic structure patterning, analytical assay component deposition, or both. In some entries not further discussed, inkjet printing plays only a "nonvital role" in μPAD fabrication. Some non-microfluidic PADs have been included into Table 3 when deemed useful to illustrate the specific potential and advantages of inkjet printing. On the other hand, μPADs with printed electrodes for purely electrochemical sensing have been excluded, since they are better discussed in the context of printed electronic structures.

An important conclusion drawn from Table 3 is that inkjet-printed (μ)PADs cover a comprehensive range of analytical applications. Since inkjet printing is compatible with various materials, its applicability to (μ)PAD fabrication compares favorably with the applicability of μPADs in general (e.g. biomedical, environmental, food quality assays). The exposure of inks to a heat pulse has caused concerns when working with fragile biomolecules in thermally actuated printers, but it has been shown experimentally that this is not necessarily an issue.[59,97–99] On the other hand, high shear forces encountered during piezoelectric ink ejection have been reported as a cause for protein damage in printing.[100] Thus, an experimental evaluation is required from case to case.

The main strength of inkjet printing as a tool for the deposition of analytical assay components lies in its flexibility and precision. Three particularly strong features of inkjet printing technology relevant to μPADs, not as easily achieved by other approaches, are briefly introduced below, before being discussed in more detail with examples in the following separate sections:

1) Precise deposition and patterning of reagents because of the picoliter-sized droplets of reagent inks, which create well-defined patterns in a wide range of features (μm to cm order) with high spatial precision.
2) Repeated printing onto an identical region (multilayered printing). Alteration of the ink between printing cycles enables the deposition of several materials in an arrangement similar to layer-by-layer (LbL) approaches.
3) Any simple desktop inkjet printer is capable of printing multiple reagents simultaneously from at least four ink cartridges in individually controlled amounts.

5.1. Precise Deposition and Patterning of Reagents

5.1.1. Position Control and Spatial Confinement

In our early studies on inkjet-printed μPADs, the effect of assay region geometry and location of reagent on colorimetric assays was investigated.[7] Colorimetric assays on μPADs often suffer from an inhomogeneous color appearance in the assay regions, as a result of reagent dissolution accompanied by continuous fluid flow, thus preventing accurate quantitative analysis by digital colorimetry. The speed and flexibility of inkjet printing allow for a relatively simple optimization of microfluidic pattern geometries and location of assay

Table 2: Common analytical assays for inkjet-printed μPADs.

Type of assay	Printed functional material	Targeted analytes	Ink composition for inkjet	
			thermal	piezoelectric
classical color indicator	chromogenic dye	ions, proteins	water (buffer)	water (buffer), viscosity modifier,[a] surfactant[b]
immunoassay	antibody	antigen	buffer	buffer, viscosity modifier, surfactant
enzyme assay	enzyme	metabolites	buffer	buffer, viscosity modifier, surfactant

[a] Glycerol and glycols are typical examples of viscosity modifiers. [b] Triton X-100 is an example of a surfactant (non-ionic) to adjust the ink surface tension.

Table 3: Reported analytical applications of inkjet-printed (μ)PADs.

Assay target	Printed features	Detection type	Detector	Printer	Analytical performance[d,e]	Reference
pH, glucose, protein	hydrophobic barrier assay region (chromogens, enzymes)	colorimetry	scanner	PicoJet-2000[a]	pH: 5–9, glucose: 2.8–28 mM, human serum albumin: 0.46–46 μM	[7]
pH human IgG mouse IgG	hydrophobic barrier test/control line (antibody, antigen)	colorimetry	scanner	PicoJet-2000[a]	human IgG: **at least 10 ng mL^{-1}**	[91]
paraoxon aflatoxin B1	assay region (enzyme-trapped silica sol-gel layer)	colorimetry	digital camera, smartphone camera	Dimatix DMP-2800[a]	paraoxon: **100 nM**, aflatoxin B1: **30 nM**	[114,115]
paraoxon, bendiocarb, carbaryl, malathion	assay region (enzyme or chromogen-trapped silica sol-gel layer)	colorimetry	digital camera	Dimatix DMP-2800[a]	paraoxon: **1 nM**, bendiocarb: **1 nM**, carbaryl: **10 nM**, malathion: **10 nM**	[116]
E. coli BL21 *E. coli* O157:H7	hydrophobic barrier, assay region (silica sol-gel layer, chromogens, oxidizing agent)	colorimetry	digital camera, scanner	Dimatix DMP-2800[a]	*E. coli* BL21: **20 cfu mL^{-1}**,[f] *E. coli* O157:H7: **5 cfu ml^{-1}**[f]	[118]
Hg^{2+}, Ag^{+}, Cu^{2+}, Cd^{2+}, Pb^{2+}, Cr^{4+}, Ni^{2+}	hydrophobic barrier, assay region (enzyme-trapped silica sol-gel layer, chromogens)	colorimetry	digital camera, scanner	Dimatix DMP-2800[a]	Hg^{2+}: **0.001**, Ag^{+}: **0.002**, Cu^{2+}: **0.020**, Cd^{2+}: **0.020**, Pb^{2+}: **0.140**, Cr^{4+}: **0.150**, Ni^{2+}: **0.230 ppm**	[117]
ATP*	assay region (enzyme-trapped silica sol-gel layer)	odor	human nose	Dimatix DMP-2800[a]	1.16 μM[g] (in buffer), 1.36 μM[g] (in Orange Punch)	[126]
pH, H_2O_2	hydrophobic barrier assay region (enzymes, chromogens)	colorimetry	scanner	Epson PX-101[b]	pH: 4–9, H_2O_2: **14.4 μM**	[84,127]
lactoferrin	hydrophobic barrier pretreatment/assay region (carbonate, metal)	fluorescence	UV hand lamps, digital camera	Epson PX-105[b], Dimatix DMP-2831[a]	covers 0.63–2.9 mg mL^{-1} (**0.30 mg mL^{-1}**)	[92]
volatile primary amines	sensing spots (dye-loaded nanoparticles)	colorimetry	scanner	Dimatix DMP-2831[a]	discrimination of n-$C_nH_{2n+1}NH_2$ (n = 1–7)	[128]
nitrite, ALP*	hydrophobic barrier assay region (enzyme, chromogen)	colorimetry	scanner	Canon Pixma ip4500[c]	nitrite (NO_2^-): 0–5 mM	[80]
DBAE*, NADH*	hydrophobic barrier	electrochemiluminescence	smartphone camera	Canon Pixma ip4500[c]	DBAE: 3 μM-5 mM (**0.9 μM**), NADH: 0.2–10 mM (**200 μM**)	[129]
nitrite, nitrate	hydrophobic barrier	colorimetry	scanner	Canon P4700[c]	nitrate (NO_2^-): 10–150 μM (**1.0 μM**, LOQ 7.8 μM), nitrate (NO_3^-): 50–1000 μM (**19 μM**, LOQ 48 μM)	[94]
nitrite, uric acid	hydrophobic barrier	colorimetry	scanner	Canon Pixma ip4500[c]	nitrite: 0–1250 μM	[130]
reactive phosphate	hydrophobic barrier	colorimetry	scanner	Canon P4700[c]	0.2–10 mg L^{-1} P (**0.05 mg L^{-1} P**, LOQ 0.16 mg L^{-1} P)	[131]
metabolic volatiles from food product	assay region (fluorescent oligomers)	fluorescence	Hg lamp, epi-fluorescence microscope	HP Deskjet F4280[c]	monitoring of meats, dairy, fruit, grain, vegetable spoilage and fruits ripening	[43]
phenolic compounds	assay region (enzyme-trapped polymer layer)	colorimetry	scanner	Dimatix DMP-2800[a]	BPA, *p*-cresol: 1–200, dopamine, catechol: 1–300, phenol: 1–400, *m*-cresol: 1–500 μg L^{-1} (**0.86 μg L^{-1}**)	[120]
hCG*	physical barrier	colorimetry	digital camera	SLT0505-HKF[a]	**1 ng mL^{-1}** in buffer solution, **4 ng mL^{-1}** in urine sample	[132]
rhodamine 6G, cocaine, heroin, malathion, BPE*	hydrophobic barrier Raman enhancer spot (silver/gold nanoparticles)	Raman spectroscopy	portable spectrometer	Epson Workforce 30[b]	rhodamine 6G: **10 fmol**, cocaine: **15 ng**, heroin: **9 ng**, malathion: **413 pg**, BPE: 1.8 **ppb**	[133–135]
2,4,6-trinitrotoluene	Raman enhancer spot (silver nanoparticles)	Raman spectroscopy	Raman spectrometer	details not available	**1.6×10^{-17} g cm^{-2}**	[136]

Table 3: (Continued)

Assay target	Printed features	Detection type	Detector	Printer	Analytical performance[d,e]	Reference
rhodamine 6G, malachite green, iprodione	Raman enhancer spot (reductant for gold nanoparticle precursor)	Raman spectroscopy	portable spectrometer	details not available	malachite green: **1 nM**, iprodione: **10 μM**	[137]
2,4,6-trinitrophenol	assay region (fluorescent nanorods)	fluorescence	UV lamp, digital camera	HP Deskjet 1000[c]	5–40 μM (**0.74 μM**) **0.45 ng mm^{-2}** (visual inspection)	[138]
volatile organic compounds	assay region (chromogen)	colorimetry, fluorescence	UV lamp, digital camera, microscope	HP Deskjet D2360[c]	discrimination of 10 organic solvent vapors	[139]
morphine	test/control line (antibodies)	colorimetry	scanner	Dimatix DMP-2831[a]	**1 ng mL^{-1}** (qualitative LOD by visual inspection)	[106]
anionic polymer, cationic surfactants	assay region (chromogen and co-factor)	colorimetry	digital camera	details not available	anionic polymer, cationic surfactants: **at least 1 mM**	[140]
glucose	assay region (enzymes)	colorimetry	spectro-photometer	Epson ME1 + [b]	0–100 mM in urine	[121]
E. coli XL1, *B. subtilius*	assay region (enzyme and substrate)	colorimetry	scanner	Epson Artisan 50[b]	*E. coli* XL1, *B. subtilius*: **10^3 cfu** (qualitative LOD by visual inspection)	[101]

[a] Piezoelectric research-use inkjet printer. [b] Piezoelectric desktop inkjet printer. [c] Thermal desktop inkjet printer. [d] The underlined value represents the linear response range. [e] The bold value represents the limit of detection (LOD). [f] If combined with immuno magnetic separation for pre-concentration. [g] BET (best estimated threshold) value. *ATP: adenosine triphosphate, ALP: alkaline phosphatase, DBAE: 2-(dibutylamino)-ethanol, NADH: nicotinamide adenine dinucleotide, hCG: human chorionic gonadotropin, BPE: 1,2-bis(4-pyridyl)ethylene.

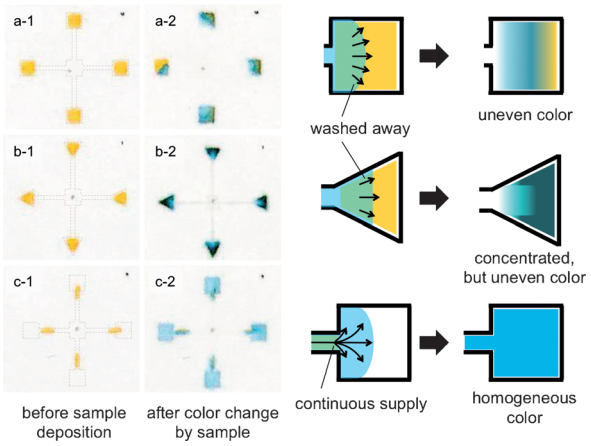

Figure 10. The geometry of the signal readout area and position of the assay reagents influence the color appearance after sample deposition. Each panel shows quadruplicate protein analysis (1) before and (2) after sample application: a) reagents in square assay areas, b) reagents in triangular assay areas, and c) reagents deposited in front of the square assay regions in the microfluidic channel (adapted from Ref. [7] with permission. Copyright 2008 American Chemical Society). The drawings on the right side show the schematic process for every case.

reagents, as shown in Figure 10 for the example of a protein assay. Compared to square assay areas (panels a-1 and a-2), triangular-shaped areas feature more intense color changes (panels b-1 and b-2), but both suffer from color inhomogeneity. On the other hand, depositing reagents in the shape of narrow lines inside the 550 μm wide microfluidic channels results in homogeneous colors in the assay areas (panels c-1 and c-2). Although all digital printing techniques enable rapid and flexible variation of the microfluidic structure on paper, only inkjet printing allows the optimization of reagent positioning with the required spatial precision (550 μm channel). Since there is no universal μPAD design and optimization is required from case to case, the flexibility and precision of inkjet printing contributes to the reproducible fabrication of μPADs with optimized performance.

A very recent example demonstrating the power of inkjet printing in terms of precise spatial control is the deposition of an enzyme and its substrate in proximity (ca. 2 mm) on paper.[101] The optimal geometry, dimensions, and reagent amounts were evaluated to prevent their mixing on the paper substrate. For this purpose, β-galactosidase and chlorophenol red-β-D-galactopyranoside (chromogenic substrate) were inkjet-printed at different concentrations and in various geometrical arrangements (diamond, weave, checkerboard, etc.). When contacted with water, which allows the diffusion of the enzyme and substrate, each pattern showed a different color appearance, which indicates different activities dependent on their layout (Figure 11).

If multiple reagents have to be immobilized on discrete regions of a single μPAD, cross-talk among adjacent components is unfavorable. A problem with the application of reagent-deposition methods other than inkjet printing is the fact that the minimal achievable droplet volumes are often significantly larger. This becomes an issue on paper-based substrates, since the presence of "excess" ink liquid results in an immediate spreading by wicking driven by the capillary force. This holds for manual pipetting of course, but also for

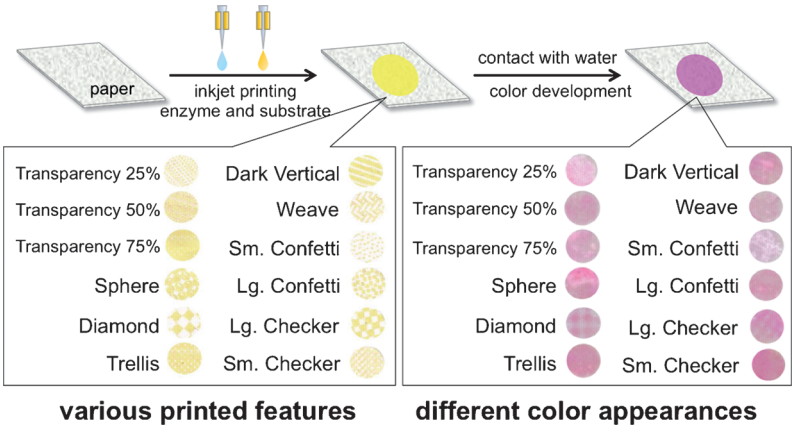

Figure 11. Printed geometrical arrangements of enzyme and substrate (left images), and subsequent appearance after chromogenic reaction by soaking in water (right images). Adapted from Ref. [101] with permission. Copyright 2014 American Chemical Society.

contact printing by pin spotting. Although the latter is theoretically able to achieve similar resolution to inkjet printing,[102] it involves the direct contact between the paper substrate and the ink-loaded dispenser. There is a concern that the capillary action of paper results in the drawing of excess ink from the orifice of the spotter. Significant reagent spreading with poor reproducibility was, for example, observed for contact printing on paper substrates (copy paper and pure cellulose chromatography paper) because of the large dispensing volume (ca. 100 nL) and capillary action by the porous substrate structure.[103]

The only simple alternative to prevent reagent spreading and mixing is to move to larger scale μPADs. However, a scale-up of μPADs is automatically accompanied by higher costs and increased sample volume requirement. Since affordability is crucial for μPADs, costs have to be minimized by saving material and optimizing manufacturing.[22,80] Surprisingly, in the case of using filter paper, the paper substrate is the dominant cost factor of μPADs,[92,104] thus efficient spatial design of microfluidic patterns is well-worth considering. The requirement for low sample volumes in the case of medical diagnostics was recently demonstrated with an antibody-free biological tear protein analysis on a μPAD.[92] The collection volume of human tear fluid is relatively low (typically 10 μL from healthy persons, <3 μL from ocular disease patients), and an accordingly compact μPAD was designed to ensure analysis from 2.5 μL of tear sample (Figure 12). In the case of manually depositing the reagents into the 3×3 mm^2 assay areas by micropipetters, the signal homogeneity was not comparable with spots obtained by inkjet printing.

5.1.2. *Test/Control Line Printing for Lateral Flow Immunoassays*

Lateral flow immunoassays (LFIAs) are familiar biochemical assays found in pregnancy tests and infectious disease diagnosis.[105] They give either qualitative (positive/negative) or quantitative (abundance of analyte) answers by the color displayed on a test line, and indicate assay completion by displaying a color on a control line. To prepare those lines, antibodies or antigens (immunoreagents) are commonly arranged in line patterns. The drawing of a clear test line is essential to realize precise and accurate quantitative assays.

Our research group evaluated constructing a LFIA on a single piece of cellulosic filter paper.[91] Microfluidic structures and test/control lines were prepared by means of inkjet printing (Figure 13a). To prevent spreading of the immunoreagents during repeated printing cycles, they were deposited on narrow line-shaped inkjet-etched regions surrounded by hydrophobic barriers, instead of completed microfluidic patterns. Although this approach calls for one additional patterning step, it is helpful to confine the reagents in well-defined areas (Figure 13b).

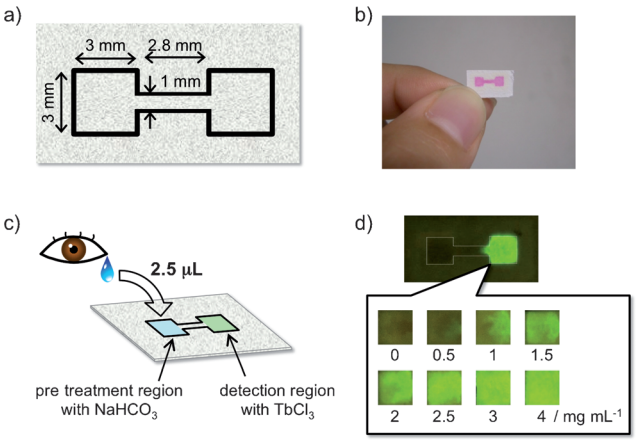

Figure 12. μPAD for the quantification of lactoferrin in human tears based on the sensitization of Tb^{3+} fluorescence emission: a) outline and dimensions; the black line indicates the hydrophobic barrier created by the inkjet printing of UV-curable ink followed by photopolymerization, b) photograph of a microfluidic pattern visualized by a food colorant solution, c) schematic depiction of the analysis of human tear fluid, and d) fluorescence signal emission from the assay region under UV illumination after deposition of calibration solutions of different concentrations. Adapted from Ref. [92] with permission from The Royal Society of Chemistry.

This line confinement approach can only be realized with etching-based microfluidic patterning methods. However, even the direct inkjet printing of immunoreagents inside a microfluidic structure still provides sharp line formation, since the small droplet volumes trigger only minimal spreading of the ejected ink on the paper. This has been shown with an LFIA for morphine by printing a recombinant anti-morphine fragment onto paper substrates.[106] Along with the above-mentioned examples, other clinically useful antibodies (e.g. anti-C-reactive protein,[107,108] anti-cholera toxin,[109] antibodies for cytokines, breast cancer biomarkers, cancer-related protein,[110] anti-tumor necrosis factor-α)[111] have successfully been deposited by inkjet printing on various substrates.

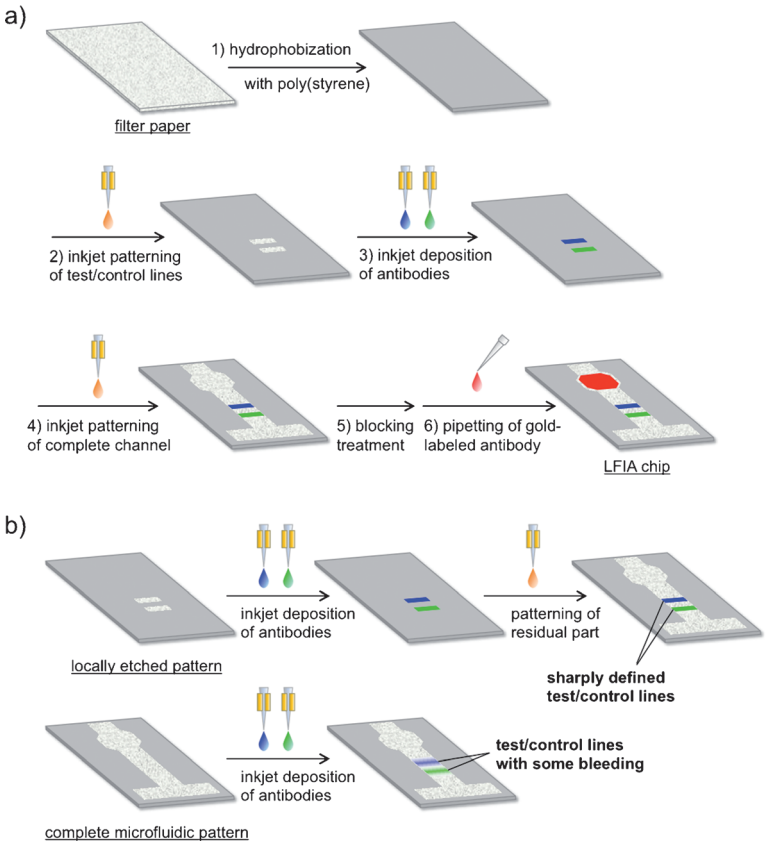

Figure 13. a) Fabrication of a inkjet-printed lateral flow immunoassay (LFIA) device on filter paper (adapted from Ref. [91] with kind permission from Springer Science and Business Media); b) printing of immunoreagents onto locally etched hydrophilic regions ahead of the microfluidic patterning gives more confined test/control lines (upper row) than printing into a prepatterned microfluidic structure (lower row).

5.2. Printing of Layered Structures

Fragile analytical assay components such as enzymes and antibodies are frequently incorporated in μPADs. The storage stability of those compounds on paper substrates is crucial when practical application is considered.

Sol-gel-derived silica is a powerful material to reinforce the robustness of biomolecules.[112] It has been known for decades that biomolecules encapsulated in hydrolyzed (and condensed) silica matrices show enhanced durability.[113] In 2009, this strategy was first transferred to protein-based PADs by the Brennan research group.[114] They referred to inkjet printing to construct a silica sol-gel assay region that entrapped an enzyme on a dipstick-type paper device. Conventionally, dip/spin coating or spraying has been used, but these techniques do not satisfy high productivity, economical reagent use, or miniaturization requirements. Direct printing of enzyme-entrapped silica material is not possible, because the gelation of the ink causes clogging of the print nozzles. Step-by-step printing of a cationically charged underlayer (poly(vinylamine) PVAm), a first silica sol-gel precursor layer, enzyme (acetylcholinesterase, AChE), and a second silica sol-gel precursor layer was confirmed to form a layered structure (Figure 14a). A detailed morphological study elucidated that the constructed layers formed tens of nanometers thin coatings of composite silica materials on the cellulose fibers.[115] This layered bio-ink structure has been adapted to develop PADs that target the detection of pesticides[114,116] and toxic heavy metals,[117] by using deactivation of the entrapped enzyme (AChE or β-galactosidase) as the signaling mechanism. Furthermore, the concept was applied to the entrapment of enzyme substrates, thereby expanding the field of application to the detection of foodborne pathogens (*E. coli* BL21 and *E. coli* O157:H7) by monitoring their intracellular enzymes.[118] Based on this concept, it can be expected that further classical enzymatic assays and other combinations of enzymes and substrates for bacterial assays[119] could be flexibly accommodated on PADs.

A similar inkjet printing based approach to a layer-by-layer structure was established for enzyme stabilization and immobilization between alternate layers of a cationic and anionic polymer.[120] Tyrosinase was deposited between cationic chitosan and anionic sodium alginate, after the printing of sodium triphosphate pentabasic (NaTPP) as a stabilizer and cross-linker of chitosan (Figure 14b). Tyrosinase entrapped by electrostatic adsorption showed excellent stability (92% residual activity after 260 days at room temperature, 99% after 54 days, and 97% after

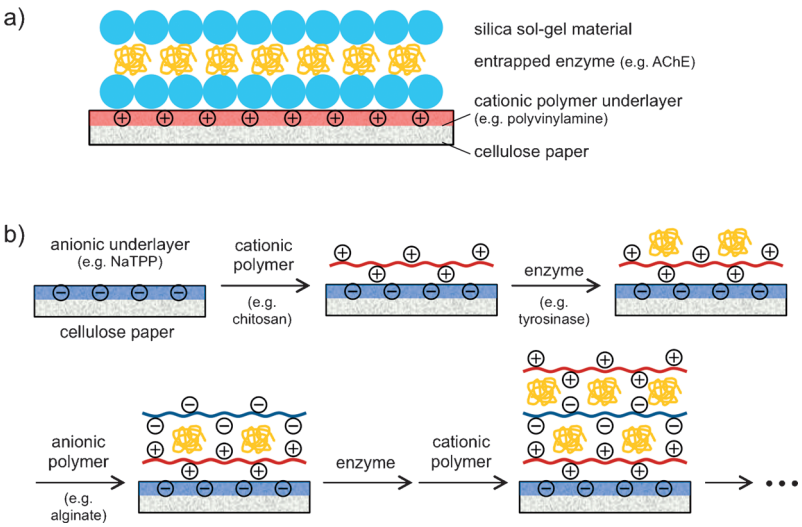

Figure 14. Strategies for enzyme entrapment and stabilization using inkjet-deposited layered structures of: a) silica sol-gel materials (adapted from Ref. [114] with permission. Copyright 2009 American Chemical Society), and b) a pair of positively/negatively charged polymer materials (adapted from Ref. [120] with permission. Copyright 2012 American Chemical Society).

260 days of refrigeration or freezing) thanks to the biocompatible microenvironment provided by the chitosan and alginate. This approach is another example of a simple fabrication method of enzyme-immobilized PADs with a prolonged shelf life.

5.3. Simultaneous Printing of Multiple Reagents

One of the most promising and useful features of common desktop inkjet printers is the availability of at least four ink reservoirs (cyan, magenta, yellow, and black), which theoretically enables simultaneous deposition of four materials. An inkjet printer does not only allow the preparation of serially diluted spots by controlling the amount of deposition for a single reagent (Figure 15a), but has the potential for on-device mixing (Figure 15b) or gradient printing (Figure 15c) of multiple components, all achieved by simple adjustment of color patterns in a graphical software. Creating a gradient of printed analytical assay components cannot be as readily achieved by any method other than inkjet printing. Surprisingly, this characteristic of inkjet printers is to date very rarely made use of in the development of μPADs.

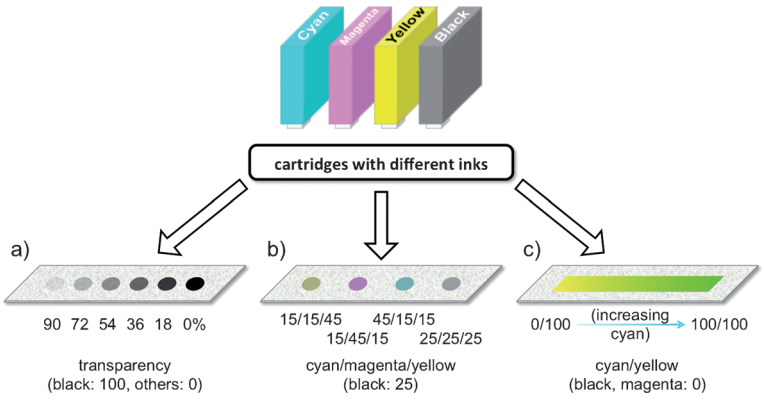

Figure 15. The configuration of the print color allows for the deposition of multiple inks with various features: a) the transparency value varies the amount of a single reagent, b) the CMYK values can independently adjust the ejection ratio from individually addressable cartridges filled with different reagents, and c) color gradient within a single graphic creates a continuously increasing (decreasing) reagent gradient.

An example, where the strategy of mixing several reagents on paper has been cleverly applied, is the high-throughput screening of the optimal molar ratio of reagents in a reaction involving multiple components, as recently demonstrated to construct multienzyme systems on paper substrates using an inkjet printer.[121] In this study, two sets of enzyme combinations (GOx/HRP, diaphrose (DP)/alcohol dehydrogenase (ADH)) were printed in different proportions to achieve the most effective bienzymatic reactions. After proving a good agreement between the preset mass ratio (CMYK color value in the graphic software) and the printed mass ratio (judged from the emission of fluorescently labeled enzymes), the enzyme ratios to obtain maximum reaction yields (GOx/HRP = 2:8, DP/ADH = 5:95) were determined (the case of

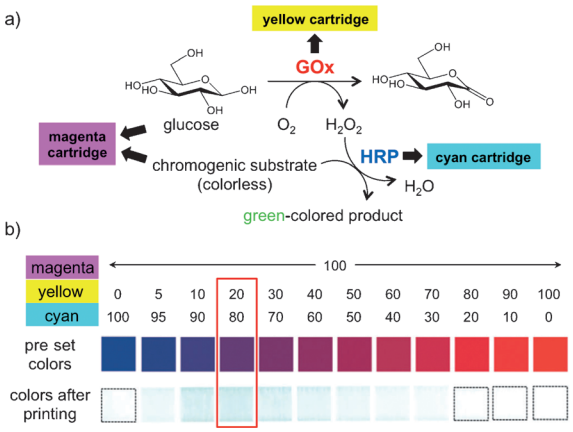

Figure 16. Optimization of reagent ratios based on simultaneous inkjet printing of materials: a) color generating bi-enzymatic system, b) preset print color and color after enzymatic reaction. The strongest color (yellow/cyan = 20:80) indicates the optimal molar ratio of GOx/HRP. Adapted from Ref. [121] with permission from The Royal Society of Chemistry.

GOx/HRP is shown in Figure 16). Thanks to the advantages of inkjet printing, the time and workload required for optimization of the enzyme ratio could be drastically reduced compared to standard enzymatic assays in solution.

6. Summary and Outlook

Although inkjet printing is a promising technology for developing highly functional μPADs, some inherent weaknesses have to be mentioned. While digital control of the printing process allows for rapid and flexible modification of print patterns, the printed image itself is built up through dot-by-dot deposition of ink droplets. Thus, the process is inherently slower than plate or screen-based printing systems, where the entire pattern is transferred to the substrate in one step. Therefore, in the case of the reproduction of large amounts of identical patterns that do not require high print resolution, inkjet printing cannot compete with other major printing techniques in terms of speed.

The limited windows of ink viscosity and surface tension occasionally diminish the versatility of the inkjet printing technique. In particular, the requirement of using surfactants in some cases might be problematic when it comes to the fabrication of μPADs based on inks with proteins prone to denaturation. In the case of nanoparticle printing, their dispersion stability in the ink vehicle and their diameter put further restriction on ink compositions.

The possibility of depositing picoliter volumes of material inks into finely tunable patterns with high spatial resolution is a unique and almost exclusive strength of inkjet printing. It has been demonstrated on multiple occasions that even ordinary desktop inkjet printers can be used to fabricate μPADs with micrometer-sized features. Combining paper-based microfluidics with the established inkjet printing of

functional materials or biomaterials,[28] creates an exciting avenue to develop devices that are not only cost-effective, but more importantly, can be realized in a short space of time. This will allow fast response to important and highly actual societal needs, such as in disease control. A recent, although not directly inkjet-related example, is the paper-based gene network with mRNA sensors, which was developed to discriminate two strains of Ebola viruses from Sudan and Zaire.[122]

Inkjet-printed μPADs are still considered to be in their infancy, thus challenges and opportunities are abundant. Ink formulation is central to inkjet printing, which demands different ink composition for every particular functional material to achieve a clog-free, consistent pattern on a paper substrate. It might be a scientist's dream to have a rheology-independent inkjet printer to accommodate the universal printing of inks with different chemical components such as proteins, organic dyes, cells, inorganic and organic nanoparticles, and other functional materials. In reality, such a technology may not be available in the near future or may not be achievable at all. Therefore, focusing on new ink chemistry and printing meaningful physical or biological microstructures (2D or 3D)[123–125] on cellulosic substrates are a more realistic immediate research direction towards an increased variety of useful functional inkjet printed μPADs.

Financial support by the Ministry of the Environment of Japan, Nestec Ltd. (Vevey, Switzerland), and the Japan Science and Technology Agency (JST-SENTAN) is kindly acknowledged.

How to cite: *Angew. Chem. Int. Ed.* **2015**, *54*, 5294–5310
Angew. Chem. **2015**, *127*, 5384–5401

[1] A. W. Martinez, S. T. Phillips, M. J. Butte, G. M. Whitesides, *Angew. Chem. Int. Ed.* **2007**, *46*, 1318–1320; *Angew. Chem.* **2007**, *119*, 1340–1342.
[2] D. M. Cate, J. A. Adkins, J. Mettakoonpitak, C. S. Henry, *Anal. Chem.* **2015**, *87*, 19–41.
[3] E. W. Nery, L. T. Kubota, *Anal. Bioanal. Chem.* **2013**, *405*, 7573–7595.
[4] H. Sirringhaus, T. Kawase, R. H. Friend, T. Shimoda, M. Inbasekaran, W. Wu, E. P. Woo, *Science* **2000**, *290*, 2123–2126.
[5] A. Teichler, J. Perelaer, U. S. Schubert, *J. Mater. Chem. C* **2013**, *1*, 1910–1925.
[6] T. Okamoto, T. Suzuki, N. Yamamoto, *Nat. Biotechnol.* **2000**, *18*, 438–441.
[7] K. Abe, K. Suzuki, D. Citterio, *Anal. Chem.* **2008**, *80*, 6928–6934.
[8] W. K. Tomazelli Coltro, C. M. Cheng, E. Carrilho, D. P. de Jesus, *Electrophoresis* **2014**, *35*, 2309–2324.
[9] M. Santhiago, E. W. Nery, G. P. Santos, L. T. Kubota, *Bioanalysis* **2014**, *6*, 89–106.
[10] C. Rozand, *Eur. J. Clin. Microbiol. Infect. Dis.* **2014**, *33*, 147–156.
[11] J. Hu, S. Wang, L. Wang, F. Li, B. Pingguan-Murphy, T. J. Lu, F. Xu, *Biosens. Bioelectron.* **2014**, *54*, 585–597.
[12] L. Ge, J. H. Yu, S. G. Ge, M. Yan, *Anal. Bioanal. Chem.* **2014**, *406*, 5613–5630.
[13] A. K. Yetisen, M. S. Akram, C. R. Lowe, *Lab Chip* **2013**, *13*, 2210–2251.
[14] W. L. Then, G. Garnier, *Rev. Anal. Chem.* **2013**, *32*, 269–294.
[15] E. J. Maxwell, A. D. Mazzeo, G. M. Whitesides, *Mrs Bull.* **2013**, *38*, 309–314.
[16] P. Lisowski, P. K. Zarzycki, *Chromatographia* **2013**, *76*, 1201–1214.
[17] S. Byrnes, G. Thiessen, E. Fu, *Bioanalysis* **2013**, *5*, 2821–2836.
[18] D. D. Liana, B. Raguse, J. J. Gooding, E. Chow, *Sensors* **2012**, *12*, 11505–11526.
[19] X. Li, D. R. Ballerini, W. Shen, *Biomicrofluidics* **2012**, *6*, 011301.
[20] D. R. Ballerini, X. Li, W. Shen, *Microfluid. Nanofluid.* **2012**, *13*, 769–787.
[21] W. K. Tomazelli Coltro, D. P. de Jesus, J. A. Fracassi da Silva, C. L. do Lago, E. Carrilho, *Electrophoresis* **2010**, *31*, 2487–2498.
[22] A. W. Martinez, S. T. Phillips, G. M. Whitesides, E. Carrilho, *Anal. Chem.* **2010**, *82*, 3–10.
[23] R. Pelton, *Trends Anal. Chem.* **2009**, *28*, 925–942.
[24] L. Gonzalez-Macia, A. Morrin, M. R. Smyth, A. J. Killard, *Analyst* **2010**, *135*, 845–867.
[25] J. T. Delaney, P. J. Smith, U. S. Schubert, *Soft Matter* **2009**, *5*, 4866–4877.
[26] E. Tekin, P. J. Smith, U. S. Schubert, *Soft Matter* **2008**, *4*, 703–713.
[27] B. J. de Gans, P. C. Duineveld, U. S. Schubert, *Adv. Mater.* **2004**, *16*, 203–213.
[28] P. Calvert, *Chem. Mater.* **2001**, *13*, 3299–3305.
[29] N. Komuro, S. Takaki, K. Suzuki, D. Citterio, *Anal. Bioanal. Chem.* **2013**, *405*, 5785–5805.
[30] M. Singh, H. M. Haverinen, P. Dhagat, G. E. Jabbour, *Adv. Mater.* **2010**, *22*, 673–685.
[31] A. Manz, N. Graber, H. M. Widmer, *Sens. Actuators B* **1990**, *1*, 244–248.
[32] D. R. Reyes, D. Iossifidis, P.-A. Auroux, A. Manz, *Anal. Chem.* **2002**, *74*, 2623–2636.
[33] P.-A. Auroux, D. Iossifidis, D. R. Reyes, A. Manz, *Anal. Chem.* **2002**, *74*, 2637–2652.
[34] P. Yager, T. Edwards, E. Fu, K. Helton, K. Nelson, M. R. Tam, B. H. Weigl, *Nature* **2006**, *442*, 412–418.
[35] G. M. Whitesides, *Nature* **2006**, *442*, 368–373.
[36] N. Blow, *Nat. Methods* **2009**, *6*, 683–686.
[37] J. L. Osborn, B. Lutz, E. Fu, P. Kauffman, D. Y. Stevens, P. Yager, *Lab Chip* **2010**, *10*, 2659–2665.
[38] L. Gervais, E. Delamarche, *Lab Chip* **2009**, *9*, 3330–3337.
[39] D. L. Clegg, *Anal. Chem.* **1950**, *22*, 48–59.
[40] R. H. Müller, D. L. Clegg, *Anal. Chem.* **1949**, *21*, 1123–1125.
[41] A. W. Martinez, S. T. Phillips, B. J. Wiley, M. Gupta, G. M. Whitesides, *Lab Chip* **2008**, *8*, 2146–2150.
[42] S. Y. Wong, M. Cabodi, J. P. Rolland, C. M. Klapperich, *Anal. Chem.* **2014**, *86*, 11981–11985.
[43] H. Kwon, F. Samain, E. T. Kool, *Chem. Sci.* **2012**, *3*, 2542–2549.
[44] S. Alila, S. Boufi, M. N. Belgacem, D. Beneventi, *Langmuir* **2005**, *21*, 8106–8113.
[45] F. Kong, Y. Hu, *Anal. Bioanal. Chem.* **2012**, *403*, 7–13.
[46] S. Su, R. Nutiu, C. D. M. Filipe, Y. Li, R. Pelton, *Langmuir* **2007**, *23*, 1300–1302.
[47] C. Tyagi, L. K. Tomar, H. Singh, *J. Appl. Polym. Sci.* **2009**, *111*, 1381–1390.
[48] Y. Zhu, X. Xu, N. D. Brault, A. J. Keefe, X. Han, Y. Deng, J. Xu, Q. Yu, S. Jiang, *Anal. Chem.* **2014**, *86*, 2871–2875.
[49] A. Yu, J. Shang, F. Cheng, B. A. Paik, J. M. Kaplan, R. B. Andrade, D. M. Ratner, *Langmuir* **2012**, *28*, 11265–11273.
[50] H. P. Le, *J. Imaging Sci. Technol.* **1998**, *42*, 49–62.
[51] L. Setti, C. Piana, S. Bonazzi, B. Ballarin, D. Frascaro, A. Fraleoni-Morgera, S. Giuliani, *Anal. Lett.* **2004**, *37*, 1559–1570.
[52] J. E. Fromm, *IBM J. Res. Dev.* **1984**, *28*, 322–333.
[53] H. C. Nallan, J. A. Sadie, R. Kitsomboonloha, S. K. Volkman, V. Subramanian, *Langmuir* **2014**, *30*, 13470–13477.

[54] J. Tai, H. Y. Gan, Y. N. Liang, B. K. Lok in *Proceedings of the 10th Electronics Packaging Technology Conference,* **2008**, pp. 761 – 766.
[55] B. Derby, *Annu. Rev. Mater. Res.* **2010**, *40*, 395 – 414.
[56] D. Jang, D. Kim, J. Moon, *Langmuir* **2009**, *25*, 2629 – 2635.
[57] M. R. N. Monton, E. M. Forsberg, J. D. Brennan, *Chem. Mater.* **2012**, *24*, 796 – 811.
[58] S. Magdassi in *The Chemistry of Inkjet Inks* (Ed.: S. Magdassi), World Scientific, Singapore, **2010**, pp. 19 – 41.
[59] S. Di Risio, N. Yan, *J. Adhes. Sci. Technol.* **2010**, *24*, 661 – 684.
[60] C. Renault, X. Li, S. E. Fosdick, R. M. Crooks, *Anal. Chem.* **2013**, *85*, 7976 – 7979.
[61] J. Nie, Y. Liang, Y. Zhang, S. Le, D. Li, S. Zhang, *Analyst* **2013**, *138*, 671 – 676.
[62] E. M. Fenton, M. R. Mascarenas, G. P. Lopez, S. S. Sibbett, *ACS Appl. Mater. Interfaces* **2009**, *1*, 124 – 129.
[63] D. Klemm, B. Heublein, H. P. Fink, A. Bohn, *Angew. Chem. Int. Ed.* **2005**, *44*, 3358 – 3393; *Angew. Chem.* **2005**, *117*, 3422 – 3458.
[64] M. A. Hubbe, *BioResources* **2006**, *2*, 106 – 145.
[65] Y. Wu, P. Xue, Y. Kang, K. M. Hui, *Anal. Chem.* **2013**, *85*, 8661 – 8668.
[66] L. OuYang, C. Wang, F. Du, T. Zheng, H. Liang, *RSC Adv.* **2014**, *4*, 1093 – 1101.
[67] Q. He, C. Ma, X. Hu, H. Chen, *Anal. Chem.* **2013**, *85*, 1327 – 1331.
[68] S. A. Klasner, A. K. Price, K. W. Hoeman, R. S. Wilson, K. J. Bell, C. T. Culbertson, *Anal. Bioanal. Chem.* **2010**, *397*, 1821 – 1829.
[69] X. Li, J. Tian, T. Nguyen, W. Shen, *Anal. Chem.* **2008**, *80*, 9131 – 9134.
[70] J. Wang, M. R. N. Monton, X. Zhang, C. D. M. Filipe, R. Pelton, J. D. Brennan, *Lab Chip* **2014**, *14*, 691 – 695.
[71] H. Yang, Q. Kong, S. Wang, J. Xu, Z. Bian, X. Zheng, C. Ma, S. Ge, J. Yu, *Biosens. Bioelectron.* **2014**, *61*, 21 – 27.
[72] M. P. Sousa, J. F. Mano, *Cellulose* **2013**, *20*, 2185 – 2190.
[73] J. Nie, Y. Zhang, L. Lin, C. Zhou, S. Li, L. Zhang, J. Li, *Anal. Chem.* **2012**, *84*, 6331 – 6335.
[74] Y. Lu, W. Shi, L. Jiang, J. Qin, B. Lin, *Electrophoresis* **2009**, *30*, 1497 – 1500.
[75] T. Songjaroen, W. Dungchai, O. Chailapakul, W. Laiwattanapaisal, *Talanta* **2011**, *85*, 2587 – 2593.
[76] Y. Sameenoi, P. N. Nongkai, S. Nouanthavong, C. S. Henry, D. Nacapricha, *Analyst* **2014**, *139*, 6580 – 6588.
[77] C. Renault, J. Koehne, A. J. Ricco, R. M. Crooks, *Langmuir* **2014**, *30*, 7030 – 7036.
[78] V. Rajendra, C. Sicard, J. D. Brennan, M. A. Brook, *Analyst* **2014**, *139*, 6361 – 6365.
[79] J. Olkkonen, K. Lehtinen, T. Erho, *Anal. Chem.* **2010**, *82*, 10246 – 10250.
[80] X. Li, J. Tian, G. Garnier, W. Shen, *Colloids Surf. B* **2010**, *76*, 564 – 570.
[81] E. Carrilho, A. W. Martinez, G. M. Whitesides, *Anal. Chem.* **2009**, *81*, 7091 – 7095.
[82] D. A. Bruzewicz, M. Reches, G. M. Whitesides, *Anal. Chem.* **2008**, *80*, 3387 – 3392.
[83] A. Määttänen, D. Fors, S. Wang, D. Valtakari, P. Ihalainen, J. Peltonen, *Sens. Actuators B* **2011**, *160*, 1404 – 1412.
[84] K. Maejima, S. Tomikawa, K. Suzuki, D. Citterio, *RSC Adv.* **2013**, *3*, 9258 – 9263.
[85] W. Dungchai, O. Chailapakul, C. S. Henry, *Analyst* **2011**, *136*, 77 – 82.
[86] P. de Tarso Garcia, T. M. Garcia Cardoso, C. D. Garcia, E. Carrilho, W. K. Tomazelli Coltro, *RSC Adv.* **2014**, *4*, 37637 – 37644.
[87] Y. Zhang, C. B. Zhou, J. F. Nie, S. W. Le, Q. Qin, F. Liu, Y. P. Li, J. P. Li, *Anal. Chem.* **2014**, *86*, 2005 – 2012.
[88] T. Nurak, N. Praphairaksit, O. Chailapakul, *Talanta* **2013**, *114*, 291 – 296.
[89] B. J. de Gans, S. Hoeppener, U. S. Schubert, *Adv. Mater.* **2006**, *18*, 910 – 914.
[90] T. Kawase, H. Sirringhaus, R. H. Friend, T. Shimoda, *Adv. Mater.* **2001**, *13*, 1601 – 1605.
[91] K. Abe, K. Kotera, K. Suzuki, D. Citterio, *Anal. Bioanal. Chem.* **2010**, *398*, 885 – 893.
[92] K. Yamada, S. Takaki, N. Komuro, K. Suzuki, D. Citterio, *Analyst* **2014**, *139*, 1637 – 1643.
[93] M. S. Li, J. F. Tian, M. Al-Tamimi, W. Shen, *Angew. Chem. Int. Ed.* **2012**, *51*, 5497 – 5501; *Angew. Chem.* **2012**, *124*, 5593 – 5597.
[94] B. M. Jayawardane, S. Wei, I. D. McKelvie, S. D. Kolev, *Anal. Chem.* **2014**, *86*, 7274 – 7279.
[95] M. Elsharkawy, T. M. Schutzius, C. M. Megaridis, *Lab Chip* **2014**, *14*, 1168 – 1175.
[96] A. M. M. Rosa, A. F. Louro, S. A. M. Martins, J. Inácio, A. M. Azevedo, D. M. F. Prazeres, *Anal. Chem.* **2014**, *86*, 4340 – 4347.
[97] L. Setti, A. Fraleoni-Morgera, I. Mencarelli, A. Filippini, B. Ballarin, M. Di Biase, *Sens. Actuators B* **2007**, *126*, 252 – 257.
[98] L. Setti, A. Fraleoni-Morgera, B. Ballarin, A. Filippini, D. Frascaro, C. Piana, *Biosens. Bioelectron.* **2005**, *20*, 2019 – 2026.
[99] M. S. Khan, D. Fon, X. Li, J. Tian, J. Forsythe, G. Garnier, W. Shen, *Colloids Surf. B* **2010**, *75*, 441 – 447.
[100] G. M. Nishioka, A. A. Markey, C. K. Holloway, *J. Am. Chem. Soc.* **2004**, *126*, 16320 – 16321.
[101] B. Creran, X. Li, B. Duncan, C. S. Kim, D. F. Moyano, V. M. Rotello, *ACS Appl. Mater. Interfaces* **2014**, *6*, 19525 – 19530.
[102] I. Barbulovic-Nad, M. Lucente, Y. Sun, M. Zhang, A. R. Wheeler, M. Bussmann, *Crit. Rev. Biotechnol.* **2006**, *26*, 237 – 259.
[103] M. K. LaGasse, J. M. Rankin, J. R. Askim, K. S. Suslick, *Sens. Actuators B* **2014**, *197*, 116 – 122.
[104] M. M. Mentele, J. Cunningham, K. Koehler, J. Volckens, C. S. Henry, *Anal. Chem.* **2012**, *84*, 4474 – 4480.
[105] V. Gubala, L. F. Harris, A. J. Ricco, M. X. Tan, D. E. Williams, *Anal. Chem.* **2012**, *84*, 487 – 515.
[106] T. Teerinen, T. Lappalainen, T. Erho, *Anal. Bioanal. Chem.* **2014**, *406*, 5955 – 5965.
[107] B. Feyssa, C. Liedert, L. Kivimaki, L.-S. Johansson, H. Jantunen, L. Hakalahti, *PLoS One* **2013**, *8*, e68918.
[108] S. Nilsson, C. Lager, T. Laurell, S. Birnbaum, *Anal. Chem.* **1995**, *67*, 3051 – 3056.
[109] J. B. Delehanty, F. S. Ligler, *Anal. Chem.* **2002**, *74*, 5681 – 5687.
[110] H. Li, R. F. Leulmi, D. Juncker, *Lab Chip* **2011**, *11*, 528 – 534.
[111] K. Abe, Y. Hashimoto, S. Yatsushiro, S. Yamamura, M. Bando, Y. Hiroshima, J.-i. Kido, M. Tanaka, Y. Shinohara, T. Ooie, Y. Baba, M. Kataoka, *PLoS One* **2013**, *8*, e53620.
[112] G. Aragay, F. Pino, A. Merkoçi, *Chem. Rev.* **2012**, *112*, 5317 – 5338.
[113] D. Avnir, S. Braun, O. Lev, M. Ottolenghi, *Chem. Mater.* **1994**, *6*, 1605 – 1614.
[114] S. M. Z. Hossain, R. E. Luckham, A. M. Smith, J. M. Lebert, L. M. Davies, R. H. Pelton, C. D. M. Filipe, J. D. Brennan, *Anal. Chem.* **2009**, *81*, 5474 – 5483.
[115] J. Wang, D. Bowie, X. Zhang, C. Filipe, R. Pelton, J. D. Brennan, *Chem. Mater.* **2014**, *26*, 1941 – 1947.
[116] S. M. Hossain, R. E. Luckham, M. J. McFadden, J. D. Brennan, *Anal. Chem.* **2009**, *81*, 9055 – 9064.
[117] S. M. Z. Hossain, J. D. Brennan, *Anal. Chem.* **2011**, *83*, 8772 – 8778.
[118] S. M. Z. Hossain, C. Ozimok, C. Sicard, S. Aguirre, M. M. Ali, Y. Li, J. Brennan, *Anal. Bioanal. Chem.* **2012**, *403*, 1567 – 1576.
[119] S. Orenga, A. L. James, M. Manafi, J. D. Perry, D. H. Pincus, *J. Microbiol. Methods* **2009**, *79*, 139 – 155.
[120] R. S. J. Alkasir, M. Ornatska, S. Andreescu, *Anal. Chem.* **2012**, *84*, 9729 – 9737.

[121] Y. Zhang, F. Lyu, J. Ge, Z. Liu, *Chem. Commun.* **2014**, *50*, 12919 – 12922.
[122] K. Pardee, A. A. Green, T. Ferrante, D. E. Cameron, A. DaleyKeyser, P. Yin, J. J. Collins, *Cell* **2014**, *159*, 940 – 954.
[123] S. Moon, S. K. Hasan, Y. S. Song, F. Xu, H. O. Keles, F. Manzur, S. Mikkilineni, J. W. Hong, J. Nagatomi, E. Haeggstrom, A. Khademhosseini, U. Demirci, *Tissue Eng. Part C* **2010**, *16*, 157 – 166.
[124] K. Cai, H. Dong, C. Chen, L. Yang, K. D. Jandt, L. Deng, *Colloids Surf. B* **2009**, *72*, 230 – 235.
[125] T. Xu, J. Jin, C. Gregory, J. J. Hickman, T. Boland, *Biomaterials* **2005**, *26*, 93 – 99.
[126] Z. Zhang, J. Wang, R. Ng, Y. Li, Z. Wu, V. Leung, S. Imbrogno, R. Pelton, J. D. Brennan, C. D. Filipe, *Analyst* **2014**, *139*, 4775 – 4778.
[127] D. Citterio, K. Maejima, K. Suzuki, in *15th International Conference on Miniaturized Systems for Chemistry and Life Sciences—μTAS*, Seattle, **2011**, pp. 2099 – 2101.
[128] T. Soga, Y. Jimbo, K. Suzuki, D. Citterio, *Anal. Chem.* **2013**, *85*, 8973 – 8978.
[129] J. L. Delaney, C. F. Hogan, J. Tian, W. Shen, *Anal. Chem.* **2011**, *83*, 1300 – 1306.
[130] X. Li, J. Tian, W. Shen, *Cellulose* **2010**, *17*, 649 – 659.
[131] B. M. Jayawardane, I. D. McKelvie, S. D. Kolev, *Talanta* **2012**, *100*, 454 – 460.
[132] A. Apilux, Y. Ukita, M. Chikae, O. Chailapakul, Y. Takamura, *Lab Chip* **2013**, *13*, 126 – 135.
[133] W. W. Yu, I. M. White, *Analyst* **2013**, *138*, 1020 – 1025.
[134] E. P. Hoppmann, W. W. Yu, I. M. White, *Methods* **2013**, *63*, 219 – 224.
[135] W. W. Yu, I. M. White, *Anal. Chem.* **2010**, *82*, 9626 – 9630.
[136] J. Wang, L. Yang, B. Liu, H. Jiang, R. Liu, J. Yang, G. Han, Q. Mei, Z. Zhang, *Anal. Chem.* **2014**, *86*, 3338 – 3345.
[137] W.-J. Liao, P. K. Roy, S. Chattopadhyay, *RSC Adv.* **2014**, *4*, 40487 – 40493.
[138] L. Hong, Q. Mei, L. Yang, C. Zhang, R. Liu, M. Han, R. Zhang, Z. Zhang, *Anal. Chim. Acta* **2013**, *802*, 89 – 94.
[139] B. Yoon, I. S. Park, H. Shin, H. J. Park, C. W. Lee, J.-M. Kim, *Macromol. Rapid Commun.* **2013**, *34*, 731 – 735.
[140] A. Swerin, I. Mira, *Sens. Actuators B* **2014**, *195*, 389 – 395.

Received: November 28, 2014
Published online: April 13, 2015

